Proceedings of the 20th International Conference on Soil Mechanics and Geotechnical Engineering– Rahman and Jaksa (Eds)

Centrifugal and theoretical modelling of cyclic laterally loaded pile in clay

Modélisation centrifuge et théorique d'un pieu cyclique chargé latéralement dans l'argile

Jian Yu, Maosong Huang, Junlin Zhu, Chenrong Zhang & Linlong Mu
Department of Geotechnical Engineering, Tongji University, China

ABSTRACT: A series of centrifuge tests are performed to investigate the lateral stiffness degradation of piles subjected to cyclic loads in clay. Besides, a T-bar cyclic penetration test is also conducted to measure the profile of the soil undrained shear strength and calibrate the cyclic softenging model of the soil. Combining the softening model and the concept of kinematic hardening, an elastic-plastic bounding surface p-y model is developed to simulate the hysteresis characteristic and lateral resistance degardation of laterally loaded piles under cyclc loading. Comparisons with the monotonic test reveals that the API p-y model would underestimate the lateral resistance while the prediction of the developed p-y model has a good agreement with the experimental measurement. The simulation results also show approximately consistent cyclic load-displacements with the model tests, which demonstrates that the developed p-y model can reasonably model the lateral stiffness degradation of a pile in clay.

RÉSUMÉ : Une série d'essais par centrifugation est effectuée pour étudier la dégradation de la rigidité latérale des pieux soumis à des charges cycliques dans l'argile. En outre, un test de pénétration cyclique sur barre en T est également effectué pour mesurer de la résistance au cisaillement non drainé du sol et calibrer le modèle d'adoucissement du sol sous charge cyclique. En prenant compte le modèle d'adoucissement et le concept d'écrouissage cinématique, un p-y modèle avec surface de délimitation élasto-plastique est développé pour simuler la caractéristique d'hystérésis et dégradation de la résistance latérale des pieux chargés latéralement sous charge cyclique. Comparaisons avec le test sous charge monotone révèle que le modèle API p-y peut sous-estimer la résistance latérale tandis que la prédiction du modèle p-y développé a un bon accord avec la mesure expérimentale. Les résultats de la simulation ont également montré que les courbes de charge-déplacement cyclique approximativement sont cohérents avec les essais, ce qui démontre que le modèle p-y peut raisonnablement modéliser la dégradation de la rigidité latérale d'un pieu dans l'argile.

KEYWORDS: Centrifuge tests; laterally loaded pile; cyclic degradation; clay; bounding-surface p-y model.

1 INTRODUCTION.

Offshore structures supported by pile foundations always encounter lateral cyclic loads due to harsh marine environment. One of the major concerns is the degradation of foundation lateral stiffness. The p-y approach after Matlock (1970) has been popular in practical engineering, in which an empirical reduction factor was introduced to model the nature of the deterioration. This ignores the effects of loading amplitude and cycle number on the pile as well as pile-soil hysteretic response. To this end, a degradation equation of the stiffness and (or) strength was proposed by Matlock et al. (1978) assuming the soil strength degraded exponentially with cycle number. Numerous similar degradation equations have been derived empirically and experimentally (Swane & Poulos 1984; Gerolymos & Gazetas 2005; Allotey & El Naggar 2008; Heidari et al. 2014). Thereafter, the degradation of soil strength was often attributed to the cumulative plastic displacement of the pile (Su & Yan 2013; McCarron 2015; Wang & Liu 2016). However, in the classical theory of soil constitutive models, cyclic degradation (or shrinkage of yield surface) is closely related to soil accumulated plastic shear strain instead of pile deformation.

Einav & Randolph (2005) developed a strain-softening model with the aid of T-bar cyclic penetration and extraction tests relating the undrained shear strength of soft clay to the accumulated plastic shear strain, which has been greatly enriched with extensive numerical and experimental studies (Hodder et al. 2009; Zhou & Randolph 2009; White et al. 2010; Taukoor et al. 2019). In addition, Zhang et al. (2011) reported an important evidence that the lateral stiffness degradation law of piles coincides well with the strength degradation caused by T-bar cyclic penetration. As a result, the strain-softening model could be applied to analyze the cyclic degradation of a lateral loaded pile.

It should be noted that Zhang et al.'s (2011) test modelled a laterally loaded rigid pile with a fixed-head condition, which has a similar motion pattern with a T-bar, resulting in a similar degradation law. Therefore, a series of centrifuge tests were performed to examine the rationality of the strain-softening model for free-head piles. Furthermore, the aforementioned degradation models are usually combined with the Masing rule or extended Masing rule (Pyke 1979) to produce p-y hysteretic curve due to its high simplicity. Note that the Masing rule does not have enough theoretical basis to further explain the cyclic response from a classical soil mechanics perspective. Therefore, this study will further construct cyclic p-y curves within the bounding surface model framework and capture the lateral stiffness degradation features of piles in undrained clay.

2 EXPERIMENTAL INVESTIGATION

2.1 *T-bar cyclic penetration test*

A T-bar penetrometer ($L_T = 20mm$, $D_T = 5mm$ in model scale, Stewart & Randolph 1991) was used at the test acceleration of 50g at the National University of Singapore geotechnical centrifuge. Malaysia Kaolin powder was made from clay slurry to normally-consolidated clay samples. Detailed soil properties can be found in Hartono (2014). A 20mm-thick surface water layer (in model scale) was maintained throughout the centrifuge tests to ensure full saturation in the clay sample. Then, T-bar penetrometer tests were carried out just before pile loading.

The net penetration resistance q of T-bar was measured, as shown in Fig. 1a. Undrained shear strength may be estimated as the ratio of net penetration resistance to the bearing capacity factor with $s_u = q/N_{T-bar}$. N_{T-bar} is taken as 10.5 as calibrated by Stewart & Randolph (1991) for a standard T-bar of intermediate roughness. The s_u idealized profile is fitted as $s_u = 1.39z$ kPa, representing typical normally-consolidated clay. Einav & Randolph (2005) initially established the shear strength degradation model given by:

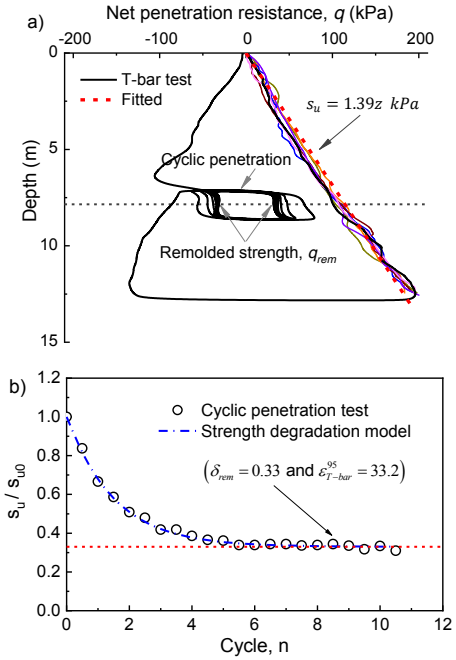

Figure 1. T-bar cyclic penetration test: (a) penetration resistance profile and (b) strength degradation versus cycles.

$$\frac{s_u}{s_{u0}} = \delta_{rem} + (1 - \delta_{rem}) exp\left(-3\frac{\varepsilon_s}{\varepsilon^{95}}\right) \quad (1)$$

where δ_{rem} is the strength ratio of fully remolded state to intact state calculated by inversing soil sensitivity; ε_s is the accumulated absolute plastic shear strain and ε^{95} is that required for 95% reduction. δ_{rem} and ε^{95} could be determined directly by experimental data (Fig. 1b) as per :

$$\frac{s_u}{s_{u0}} = \delta_{rem} + (1 - \delta_{rem}) exp\left(-3\frac{2n\varepsilon_{T-bar}}{\varepsilon^{95}_{T-bar}}\right) \quad (2)$$

where ε_{T-bar} was defined by Einav & Randolph (2005) as the average magnitude of plastic shear strain experienced by soil elements upon passing of each T-bar penetration passage. A rough value of ε_{T-bar} was estimated to be 3.7 by Zhou & Randolph (2009) following upper-bound theorem. Hence, δ_{rem} and ε^{95}_{T-bar} are fitted using Eq. 2 to be 0.33 and 33.2, respectively.

2.2 *Lateral loading test*

Rigid model pile was fabricated to simulate a monopile with a diameter of D = 2m and an embedment depth of L = 12m. Physical properties of both prototype and model piles are summarized in Table 1. The lateral load was imposed through a hinge connection to model the free head. Figure 2 illustrates the centrifuge model setup.

Table 1. Physical proprieties of prototype and model pile

Parameters	*Prototype pile*	*Model pile*
L (m)	12	0.24
D (m)	2	0.04
e (m)	2	0.04
t_p (mm)	50	1.2
E_pI_p (MNm^2)	2.9×10^4	5.5×10^{-3}

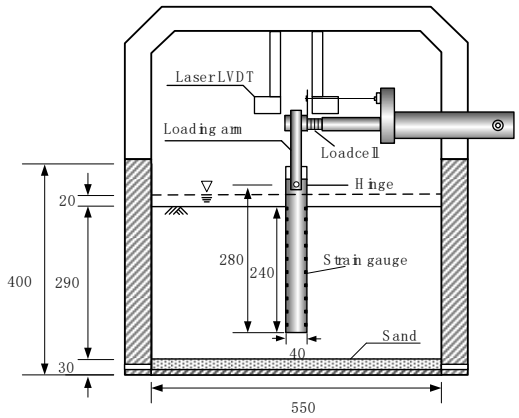

Figure 2. Schematic of model instrumentation.

The entire pile-head load-displacement data was recorded. To observe the cyclic degradation phenomenon of a laterally loaded pile, the lateral stiffness is back-calculated as pile head load P to displacement amplitude y_{max}. As Zhang et al.'s (2011) tests show a close association between soil strength and pile lateral stiffness with their plastic displacements, Fig. 3 illustrates the measured relationship of the lateral stiffness versus normalized pile head cumulative plastic displacement y^p/D. It can be seen that the lateral stiffness degrades with the increase of cumulative plastic displacement under six displacement-control tests (Test 1 is the monotonic test and not shown here). However, Fig. 3 still does not show a consistent degradation law. Therefore, the finding of Zhang et al. (2011) is only valid for the pile with lateral rigid translation. To further investigate the inner link between the soil softening with the degradation of a free-head pile reaction forces, the ratios P/P_{rem} (P_{rem} is the remoulded pile head load) in six displacement-control tests are replotted against y^p/D in Fig. 4.

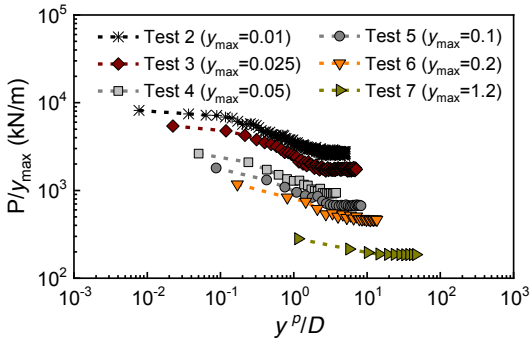

Figure 3. Measured lateral stiffness degradation under displacement-control loading.

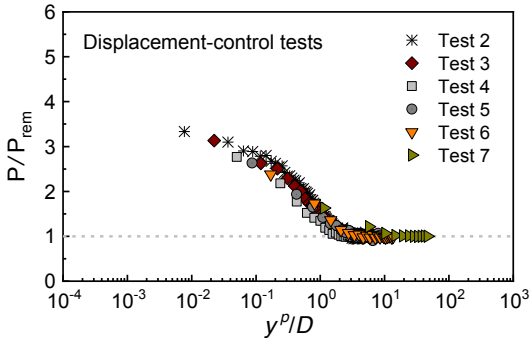

Figure 4. Degradation law of pile cyclic loading tests.

Fig. 4 reveals that the ratios P/P_{rem} in different tests have an approximately consistent degradation. Considering that the soil around the pile under these small cyclic amplitudes has a similar

motion pattern, from the view of the upper bound theory, the degradation of P/P_{rem} represents the soil strength softening of $s_u/s_{u,rem}$ ($s_{u,rem} = \delta_{rem} s_{u0}$). Therefore, the tests results demonstrate that the softening model can be used to predict the degradation of the reaction force.

2.3 *Calibration of softening parameter*

However, as mentioned earlier, ε_{T-bar} is derived in terms of the upper bound strain path approach relying on the constructed failure mechanism. Correspondingly, ε_{T-bar}^{95} is also dependent on that mechanism. As such, ε_{T-bar}^{95} requires further calibration to be ε_{pile}^{95} for laterally loaded piles.

The modification equation $\varepsilon_{pile}^{95} = 0.625 \frac{d\bar{\varepsilon}_s}{dy_{p,av}/D} \varepsilon_{T-bar}^{95}$ was established by Yu et al. (2017), where $d\bar{\varepsilon}_s$ is the incremental average maximum shear strain of the soil elements due to the average plastic pile lateral movement $dy_{p,av}/D$. Klar (2008) suggested that the ratio $\frac{d\bar{\varepsilon}_s}{dy_{p,av}/D}$ can be calculated through the upper-bound velocity field of a specific laterally loaded pile. Based on the upper-bound limit analysis of Yu et al. (2015), the ratio is estimated as around 0.158. ε_{pile}^{95} is finally modified to be 3.27. The detailed interpretation on the modification process can be found in Yu et al. (2017). Thereinafter, ε^{95} refers to ε_{pile}^{95}, unless stated otherwise.

3 BOUNDING-SURFACE-BASED P-Y MODEL

3.1 *Virgin loading*

Except for the degradation behavior, p-y hysteretic curves of piles under short-term cycle always attract attention. In soil constitutive models, it is a usual practice to employ the elastoplastic bounding surface model to capture soil hysteretic response. Hence, an attempt is made to develop a cyclic p-y model for laterally loaded piles within the concept of bounding surface model. One important assumption is that the conventional bounding surface model could be performed on p-y level by replacing the stress σ and strain ε with p and y, respectively.

In terms of the single bounding surface model proposed by Dafalias (1977), the yield and loading surfaces degenerate into a single point σ (p in this study), where plastic deformation occurs whenever pile displacement takes place. As shown in Fig. 5, for the virgin loading process, it enters elastoplastic response for soil spring from the outset of loading. Along with loading, the bounding surface p_B expands progressively, i.e. the isotropic hardening rule is adopted. Accordingly, the plastic hardening modulus H_p (or bounding surface plastic modulus H_B) decreases gradually. A limiting size p_u is given to the bounding surface to represent the limit soil resistance of laterally loaded piles.

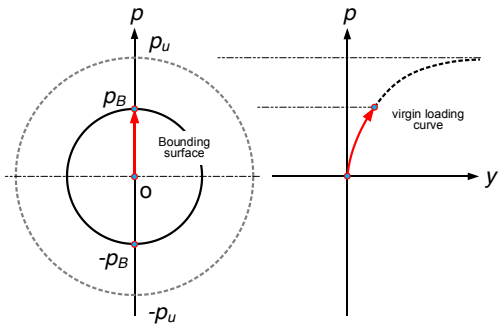

Figure 5. Bounding surface p-y model for virgin loading.

Following the concept, an elastoplastic p-y backbone curve is first required. Herein, the analytical monotonic p-y curve of Yu et al. (2017) derived from Klar (2008) is adopted. The form is theoretically deduced based on the MSD approach (Osman & Bolton 2005), and will be verified later with the experimental results, which can be rewritten as follow:

$$\frac{p}{p_u} = \frac{1}{4}\left[2 + 3\frac{f_g}{M_c} + 2f_g I_r \frac{y}{D} - \sqrt{\left(2 + 3\frac{f_g}{M_c} + 2f_g I_r \frac{y}{D}\right)^2 - 16 f_g I_r \frac{y}{D}}\right] \tag{3}$$

where p_u is the soil ultimate resistance, equaling to $N_p s_u D$; I_r is the soil rigidity factor as per E_s/s_u; $f_g = \frac{M_c \kappa}{M_c N_p - 1.5\kappa}$ serves as the group factor consisting of ultimate bearing capacity N_p, normalized initial subgrade modulus factor $\kappa = K_{in}/E_s$ and compatibility factor M_c. M_c will be illustrated in later subsection.

The elastoplastic stiffness k_{ep} of pile-soil interaction can be obtained from the p-y curve given in Eq. 3. Considering the elastic component k_e equaling to the initial subgrade modulus K_{in}, the plastic component could be expressed as:

$$H_p (or\ H_B) = \frac{2M_c N_p}{3\kappa} \frac{(p_u/p-1)^2}{2p_u/p-1} k_e \tag{4}$$

The plastic hardening modulus H_p is associated with current soil resistance p. The derivation process is provided in Yu et al. (2020).

3.2 *Cyclic rule and softening*

Upon unloading, the soil resistance would move into the bounding surface. Therefore, the plastic hardening modulus during cyclic loading process is determined with a mapping rule. Referring to the conventional bounding surface constitutive model, where the hardening modulus H_p is not only dependent on the location of the image point but also is a function of the distance from current stress point to the bounding surface, the plastic stiffness of soil spring within the bounding surface p_B is determined as per:

$$H_p = \frac{2M_c N_p}{3\kappa} \frac{(p_u/p_B \cdot b-1)^2}{2p_u/p_B \cdot b-1} k_e \tag{5}$$

where b is a geometric similarity ratio, ranging from ∞ to 1 for soil resistance moving from p_B to $-p_B$, as illustrated in Fig. 6. As one-dimensional p-space loading and unloading is easily defined by the direction of pile head load, the radial mapping (Dafalias 1976) is employed in a simple way :

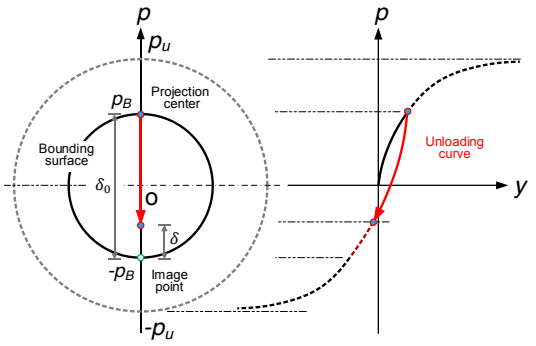

Figure 6. Mapping rule during unloading.

$$b = \frac{\delta_0}{\delta_0 - \delta} \tag{6}$$

where δ_0 and δ denote the distances from the image point to the projection center and the current loading point p, respectively (as shown in Fig. 6).

The reloading process is similar to the unloading one but the projection center p_c is updated with the current soil resistance p at each 'p reversal' to map the current reaction force p to the image point on the bounding surface, so-called moving projection center (Seidalinov & Taiebat 2013).

The softening of soil resistance during laterally cyclic loading is modelled using a softening parameter S_p according to:

$$S_p = \frac{p_u}{p_{u,rem}} = \frac{s_u}{s_{u,rem}} \tag{7}$$

where $p_{u,rem}$ is the limiting lateral resistance of the fully remolded soil, also equivalent to $\delta_{rem} N_p s_u D$. S_p is calculated by the modified form of Eq. 1, in which the accumulated absolute plastic shear strain ε_s can be calculated as

$$\varepsilon_s = 2M_c \frac{\int dy^p}{D} \tag{8}$$

where M_c is the compatibility factor representing the soil shear strain level caused by the pile movement. Eq. 8 was deduced based on upper-bound analysis performed by Klar (2008) and Yu et al. (2017) and cleared the link between soil strain and pile motion from the theoretical perspective.

The strain-displacement compatibility factor M_c was deduced to be 1.3 (Klar 2008) by upper-bound analysis, and afterward reduced to be 0.8 (Yu et al. 2017) by constructing a more reasonable plane-strain continuous mechanism. Li et al. (2020) further found M_c has three-dimensional effect (M_c varies with depth) by the limit analyses on a three-dimensional continuous mechanism.

With the increase in accumulated plastic strain, which causes a reduction of S_p, the limiting size p_u contracts gradually. Meanwhile, the bounding surface p_B decreases proportionately with p_u, with the ratio p_B/p_u maintained constant. As such, the plastic hardening modulus decreases cycle by cycle, whereas the similarity ratio b guarantees gradual decrease of H_p during each single episode of cyclic loading.

It should be noted that the projection center p_c might be found outside the bounding surface due to the contraction, which is not permitted. This will be achieved by allowing the p_c to move inside the bounding surface, with reference to Seidalinov & Taiebat (2013).

3.3 *P-y model validation*

The proposed bounding-surface-based p-y model was combined with the N_p expression of Yu et al. (2015), which is fitted from the best upper-bound solution, and the K_{in} expression of Zhang et al. (2016) modified from Vesic subgrade modulus. Fig. 7 shows the comparison of monotonic load-displacement curve at the pile head. It is evident that API underestimates the capacity of laterally loaded pile, while a good agreement between simulation result and experimental measurement demonstrates the adopted monotonic p-y curve (Eq. 3) is reasonable.

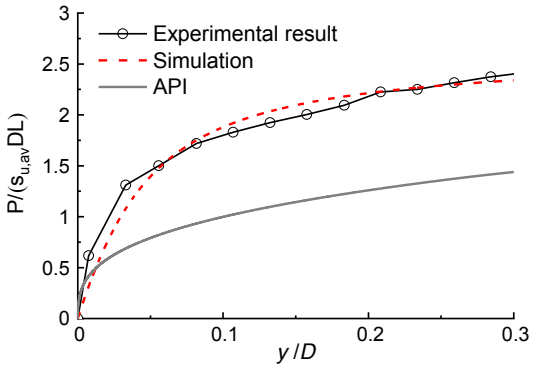

Figure 7. Load-displacement comparison for monotonic loading.

The present bounding-surface p-y model is verified through modeling cyclic load-displacement curves, for which the load-displacement hysteretic curves with a displacement amplitude of 0.1D is selected, as shown in Fig. 8. Excellent simulation is obtained.

The evolution of the normalized lateral stiffness is also captured to decrease with cycles, as illustrated in Fig. 9. The lateral stiffness degradation of varying amplitude is investigated and simulated. Apparently, the simulated results correlate well the experimental data, which demonstrates that the proposed p-y model along with the strain-softening equation given in Eq. 1 can be used to predict the degradation behavior of free-head laterally loaded pile.

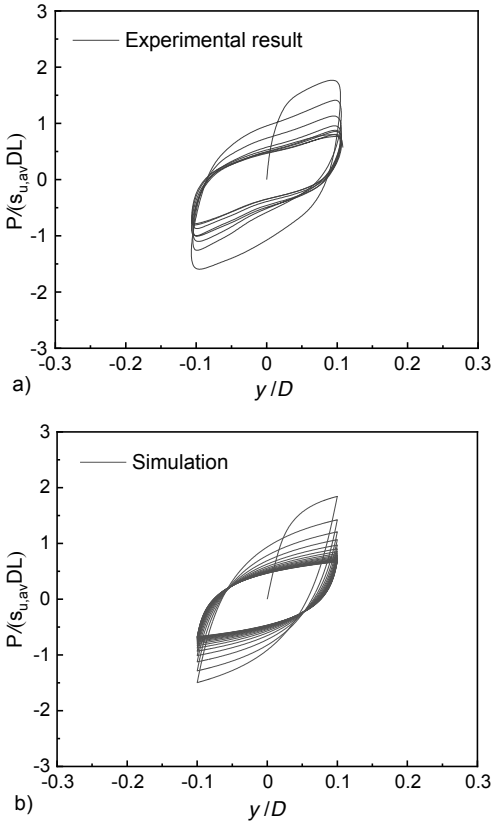

Figure 8. Load-displacement hysteretic curve: (a) experimental result and (b) simulated result.

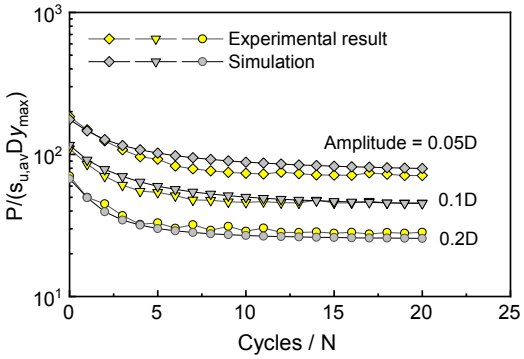

Figure 9. Lateral stiffness degradation.

4 CONCLUSIONS

A series of centrifuge tests including T-bar and pile cyclic loading have been performed to investigate the cyclic degradation of laterally loaded piles in clay. The strain-softening model is calibrated and applied to analyze a free-head monopile. Experimental evidence shows a relatively consistent trend between the softening model curve and the degradation law of pile.

Based on the observation, a cyclic p-y curve model is further developed within the framework of the bounding-surface elastoplastic theory. Comparisons of p-y hysteretic curves and the lateral stiffness degradation provide a strong evidence on the rationality of the proposed model.

This study argues that it is necessary to clear the cyclic degradation which is associated with soil accumulated plastic shear strain as opposed to pile displacement or the number of cycles. As such, the hysteresis characteristic is modeled and explained from a relatively classical soil mechanics perspective. It is anticipated that the present work will promote an accurate understanding of pile-soil cyclic response.

5 ACKNOWLEDGEMENTS

This work was financially supported by the National Natural Science Foundation of China (Grant Nos. 51908420, 51579177). These supports are gratefully acknowledged.

6 REFERENCES

Allotey, N., and El Naggar, M.H. 2008. Generalized dynamic Winkler model for nonlinear soil–structure interaction analysis. *Canadian Geotechnical Journal* 45 (4), 560-573.

Dafalias, Y.F., and Popov, E.P. 1976. Plastic internal variables formalism of cyclic plasticity. *Journal of Appllied Mechanics ASME* 645–51.

Dafalias, Y.F., and Popov, E.P. 1977. Cyclic loading for materials with a vanishing elastic region. *Nuclear Engineering and Design* 41 (2), 293-302.

Einav, I., and Randolph, M.F. 2005. Combining upper bound and strain path methods for evaluating penetration resistance. *International Journal for Numerical Methods in Engineering* 63 (14), 1991-2016.

Gerolymos, N., and Gazetas, G. 2005. Phenomenological model applied to inelastic response of soil-pile interaction systems. *Soils and Foundations* 45 (4), 119-132.

Hartono. 2014. Centrifuge model study on spudcan-footprint remediation techniques. *PhD. Thesis, National University of Singapore*, Singapore.

Heidari, M., El Naggar, H., and Jahanandish, M., et al. 2014. Generalized cyclic p–y curve modeling for analysis of laterally loaded piles. *Soil Dynamics and Earthquake Engineering* 63, 138-149.

Hodder, M.S., White, D.J., and Cassidy, M.J. 2009. Analysis of Soil Strength Degradation during Episodes of Cyclic Loading, Illustrated by the T-Bar Penetration Test. *International Journal of Geomechanics* 10 (3), 117-123.

Klar, A. 2008. Upper bound for cylinder movement using "elastic" fields and its possible application to pile deformation analysis. *International Journal of Geomechanics* 8 (2), 162-167.

Li, S., Yu, J., Huang, M., and Leung, C.F. 2020. Application of T-EMSD based p-y curves in the three-dimensional analysis of laterally loaded pile in undrained clay. *Ocean Engineering* 206.

Matlock, H. 1970. Correlations for design of laterally loaded piles in soft clay. *In: Proceedings, Offshore Technology Conference*, Houston, Texas, 577–594.

Matlock, H., Foo, S.H.C., and Bryant, L.M. 1978. Simulation of lateral pile behavior under earthquake motion. *In: Proceeding, Earthquake Engineering and Soil Dynamics ASCE*, Reston. 600–619.

McCarron, W.O. 2015. Bounding surface model for soil resistance to planar cyclic lateral pile displacements. *Computers and Geotechnics* 65, 285-290.

Osman, A.S., and Bolton, M.D. 2005. Simple plasticity-based prediction of the undrained settlement of shallow circular foundations on clay. *Géotechnique* 55 (6), 435-447.

Pyke, R. 1979. Non-linear soil models for Irregular cyclic loadings. *Journal of the Geotechnical Engineering Division-ASCE* 105 (6), 715-726.

Seidalinov, G., and Taiebat, M. 2013. Bounding surface SANICLAY plasticity model for cyclic clay behavior. *International Journal for Numerical and Analytical Methods in Geomechanics* 38 (7), 702-724.

Stewart, D. P., and M. F. Randolph. 1991. A new site investigation tool for the centrifuge. *Proceeding of international conference on geotechnical centrifuge modelling, Centrifuge* 91, Balkema, Rotterdam, Netherlands.

Su, D., and Yan, W.M. 2013. A multidirectional p–y model for lateral sand–pile interactions. *Soils and Foundations* 53 (2), 199-214.

Swane, I.C., and Poulos, H.G. 1984. Shakedown analysis of a laterally loaded pile tested in stiff clay. *In: Proceedings of 4th Australia-New Zealand Conference on Geomechanics*, Australia, 275–279.

Taukoor, V., Wallace, J.F., Rutherford, C.J., and Bernard, B.B., et al. 2019. Modelling the degradation of penetration resistance during cyclic T-bar tests in a Gulf of Mexico clay. *Soils and Foundations* 59 (6), 2331-2340.

Wang, T. and Liu, W. 2016. Development of cyclic p-y curves for laterally loaded pile based on T-bar penetration tests in clay. *Canadian Geotechnical Journal* 53 (10), 1731-1741.

White, D.J., Gaudin, C., and Boylan, N., et al. 2010. Interpretation of T-bar penetrometer tests at shallow embedment and in very soft soils. *Canadian Geotechnical Journal* 47 (2), 218-229.

Yu, J., Huang, M., and Li, S., et al. 2017a. Load-displacement and upper-bound solutions of a loaded laterally pile in clay based on a total-displacement-loading EMSD method. *Computers and Geotechnics* 83, 64-76.

Yu, J., Huang, M., and Zhang, C. 2015. Three-dimensional upper-bound analysis for ultimate bearing capacity of laterally loaded rigid pile in undrained clay. *Canadian Geotechnical Journal* 52 (11), 1775-1790.

Yu, J., Leung, C.F., and Huang, M., et al. 2017b. Application of T-bar in numerical simulations of a monopile subjected to lateral cyclic load. *Marine Georesources & Geotechnology* 36 (6), 643-651.

Yu, J., Zhu, J., Shen, K., and Huang, M., et al. 2020. Bounding-surface-based p-y model for laterally loaded piles in undrained clay. *Ocean Engineering* 216, 107997.

Zhang, C., White, D., and Randolph, M. 2011. Centrifuge modeling of the cyclic lateral response of a rigid pile in soft clay. *Journal of Geotechnical and Geoenvironmental Engineering* 137 (7), 717-729.

Zhang, C., Yu, J., and Huang, M. 2016. Winkler load-transfer analysis for laterally loaded piles. *Canadian Geotechnical Journal* 53 (7), 1110-1124.

Zhou, H., and Randolph, M.F. 2009. Resistance of full-flow penetrometers in rate-dependent and strain-softening clay. *Géotechnique* 59 (2), 79-86.